



## Article

# New arsenate minerals from the Arsenatnaya fumarole, Tolbachik volcano, Kamchatka, Russia. XIV. Badalovite, $\text{NaNaMg}(\text{MgFe}^{3+})(\text{AsO}_4)_3$ , a member of the alluaudite group

Igor V. Pekov<sup>1\*</sup>, Natalia N. Koshlyakova<sup>1</sup>, Atali A. Agakhanov<sup>2</sup>, Natalia V. Zubkova<sup>1</sup>, Dmitry I. Belakovskiy<sup>2</sup>, Marina F. Vigasina<sup>1</sup>, Anna G. Turchkova<sup>1</sup>, Evgeny G. Sidorov<sup>3</sup> and Dmitry Yu. Pushcharovsky<sup>1</sup>

<sup>1</sup>Faculty of Geology, Moscow State University, Vorobievsky Gory, 119991 Moscow, Russia; <sup>2</sup>Fersman Mineralogical Museum of the Russian Academy of Sciences, Leninsky Prospekt 18-2, 119071 Moscow, Russia; and <sup>3</sup>Institute of Volcanology and Seismology, Far Eastern Branch of Russian Academy of Sciences, Piip Boulevard 9, 683006 Petropavlovsk-Kamchatsky, Russia

### Abstract

The new alluaudite-group mineral badalovite was found in the Arsenatnaya fumarole at the Second scoria cone of the Northern Breakthrough of the Great Tolbachik Fissure Eruption, Tolbachik volcano, Kamchatka, Russia. It is associated with hematite, tenorite, cassiterite, johillerite, nickenichite, calciojohillerite, bradaczekite, metathénardite, apthitalite, langbeinite, calciolangbeinite, sanidine, fluorophlogopite, fluoborite, tilasite, anhydrite, pseudobrookite, sylvite, halite, lammerite, urusovite, ericlxmanite, arsmirandite, svabite, krashennikovite, euchlorine, wulffite and alumoklyuchevskite. Badalovite forms oblique-angled prismatic crystals up to 1 mm × 1 mm × 5 mm, typically combined in groups or crusts up to several hundred cm<sup>2</sup> in area. The mineral is transparent, green, grey, yellow or colourless, with vitreous lustre. It is brittle, the Mohs hardness is 3½. Cleavage was not observed, the fracture is uneven.  $D_{\text{calc}}$  is 4.02 g cm<sup>-3</sup>. Badalovite is optically biaxial (–),  $\alpha = 1.753(3)$ ,  $\beta = 1.757(3)$ ,  $\gamma = 1.758(3)$  and  $2V_{\text{meas.}} = 50(10)^\circ$ . Chemical composition (wt.%, electron-microprobe; holotype) is: Na<sub>2</sub>O 9.23, K<sub>2</sub>O 0.19, CaO 2.04, MgO 13.78, MnO 0.31, CuO 0.12, ZnO 0.24, Al<sub>2</sub>O<sub>3</sub> 0.06, Fe<sub>2</sub>O<sub>3</sub> 12.77, TiO<sub>2</sub> 0.01, SiO<sub>2</sub> 0.06, P<sub>2</sub>O<sub>5</sub> 0.33, V<sub>2</sub>O<sub>5</sub> 0.05, As<sub>2</sub>O<sub>5</sub> 61.51, SO<sub>3</sub> 0.02, total 100.72. The empirical formula based on 12 O apfu is Na<sub>1.67</sub>Ca<sub>0.20</sub>K<sub>0.02</sub>Mg<sub>1.92</sub>Zn<sub>0.02</sub>Mn<sub>0.02</sub>Cu<sub>0.01</sub>Fe<sub>0.90</sub><sup>3+</sup>Al<sub>0.01</sub>(As<sub>3.01</sub>P<sub>0.03</sub>Si<sub>0.01</sub>)<sub>Σ3.05</sub>O<sub>12</sub>. The simplified formula is Na<sub>2</sub>Mg<sub>2</sub>Fe<sup>3+</sup>(AsO<sub>4</sub>)<sub>3</sub>. Badalovite is monoclinic, C2/c,  $a = 11.9034(3)$ ,  $b = 12.7832(2)$ ,  $c = 6.66340(16)$  Å,  $\beta = 112.523(3)^\circ$ ,  $V = 936.59(4)$  Å<sup>3</sup> and  $Z = 4$ . The strongest reflections of the powder XRD pattern [ $d, \text{Å}(I)(hkl)$ ] are: 6.41(38)(020), 5.505(20)(200), 3.577(23)( $\bar{1}31$ ), 3.523(25)(310), 3.211(46)( $\bar{1}12$ ), 2.911(28)( $\bar{2}22$ ,  $\bar{3}12$ ), 2.765(100)(240, 400) and 2.618(26)( $\bar{1}32$ ). The crystal structure was solved from single-crystal XRD data with an  $R_1$  of = 2.49%. Badalovite is isostructural with other alluaudite-group minerals. Its simplified crystal chemical formula is  ${}^{A(1)}\text{Na}{}^{A(1)}\square{}^{A(2)}\square{}^{A(2)}\text{Na}{}^{M(1)}\text{Mg}{}^{M(2)}(\text{Mg}_{0.5}\text{Fe}_{0.5}^{3+})_2(\text{AsO}_4)_3$  ( $\square$  – vacancy) and the end-member formula is  $\text{NaNaMg}(\text{MgFe}^{3+})(\text{AsO}_4)_3$ . The mineral is named in honour of the outstanding mineralogist and geochemist Stepan Tigranovich Badalov (1919–2014).

**Keywords:** badalovite, new mineral, alluaudite group, arsenate, crystal structure, fumarole sublimate, Tolbachik volcano, Kamchatka

(Received 6 April 2020; accepted 18 May 2020; Accepted Manuscript published online: 22 May 2020; Associate Editor: Anthony R Kampf)

### Introduction

This paper continues the series of articles on new arsenate minerals from the Arsenatnaya fumarole located at the apical part of the Second scoria cone of the Northern Breakthrough of the Great Tolbachik Fissure Eruption 1975–1976, Tolbachik volcano, Kamchatka Peninsula, Far-Eastern Region, Russia (55°41'N, 160°14'E, 1200 m asl). Sixteen new species have been characterised in previous articles in the series: yurmarinite Na<sub>7</sub>(Fe<sup>3+</sup>, Mg, Cu)<sub>4</sub>(AsO<sub>4</sub>)<sub>6</sub> (Pekov *et al.*, 2014a), two polymorphs of Cu<sub>4</sub>O (AsO<sub>4</sub>)<sub>2</sub>, ericlxmanite and kozyrevskite (Pekov *et al.*, 2014b), popovite Cu<sub>5</sub>O<sub>2</sub>(AsO<sub>4</sub>)<sub>2</sub> (Pekov *et al.*, 2015a), structurally related shchurovskyite K<sub>2</sub>CaCu<sub>6</sub>O<sub>2</sub>(AsO<sub>4</sub>)<sub>4</sub> and dmsokolovite

K<sub>3</sub>Cu<sub>5</sub>AlO<sub>2</sub>(AsO<sub>4</sub>)<sub>4</sub> (Pekov *et al.*, 2015b), katiarsite KTiO(AsO<sub>4</sub>)<sub>4</sub> (Pekov *et al.*, 2016b), melanarsite K<sub>3</sub>Cu<sub>7</sub>Fe<sup>3+</sup>O<sub>4</sub>(AsO<sub>4</sub>)<sub>4</sub> (Pekov *et al.*, 2016c), pharmazincite KZnAsO<sub>4</sub> (Pekov *et al.*, 2017), arsenowagnerite Mg<sub>2</sub>(AsO<sub>4</sub>)F (Pekov *et al.*, 2018b), arsenatrotitanite NaTiO(AsO<sub>4</sub>) (Pekov *et al.*, 2019a), the two isostructural minerals edtollite K<sub>2</sub>NaCu<sub>5</sub>Fe<sup>3+</sup>O<sub>2</sub>(AsO<sub>4</sub>)<sub>4</sub> and alumoedtollite K<sub>2</sub>NaCu<sub>5</sub>AlO<sub>2</sub>(AsO<sub>4</sub>)<sub>4</sub> (Pekov *et al.*, 2019b), anatolyite Na<sub>6</sub>(Ca, Na)(Mg, Fe<sup>3+</sup>)<sub>3</sub>Al(AsO<sub>4</sub>)<sub>6</sub> (Pekov *et al.*, 2019c), zubkovaite Ca<sub>3</sub>Cu<sub>3</sub>(AsO<sub>4</sub>)<sub>4</sub> (Pekov *et al.*, 2019d) and pansnerite K<sub>3</sub>Na<sub>3</sub>Fe<sub>6</sub><sup>3+</sup>(AsO<sub>4</sub>)<sub>8</sub> (Pekov *et al.*, 2020).

Alluaudite-group arsenates in the Arsenatnaya fumarole are diverse and, in some areas, abundant (Pekov *et al.*, 2018a). In the present paper we characterise a new member of this group badalovite  $\text{NaNaMg}(\text{MgFe}^{3+})(\text{AsO}_4)_3$  (Cyrillic: бадаловит). It is named in honour of the outstanding mineralogist and geochemist Professor Stepan Tigranovich Badalov (1919–2014) who worked in the Abdullaev Institute of Geology and Geophysics, Uzbekistan Academy of Sciences, Tashkent. Prof. Badalov was an Honorary member of the Russian Mineralogical Society.

\*Author for correspondence: Email: igorpekov@mail.ru

Cite this article: Pekov I.V., Koshlyakova N.N., Agakhanov A.A., Zubkova N.V., Belakovskiy D.I., Vigasina M.F., Turchkova A.G., Sidorov E.G. and Pushcharovsky D.Y.u. (2020) New arsenate minerals from the Arsenatnaya fumarole, Tolbachik volcano, Kamchatka, Russia. XIV. Badalovite,  $\text{NaNaMg}(\text{MgFe}^{3+})(\text{AsO}_4)_3$ , a member of the alluaudite group. *Mineralogical Magazine* 84, 616–622. <https://doi.org/10.1180/mgm.2020.43>

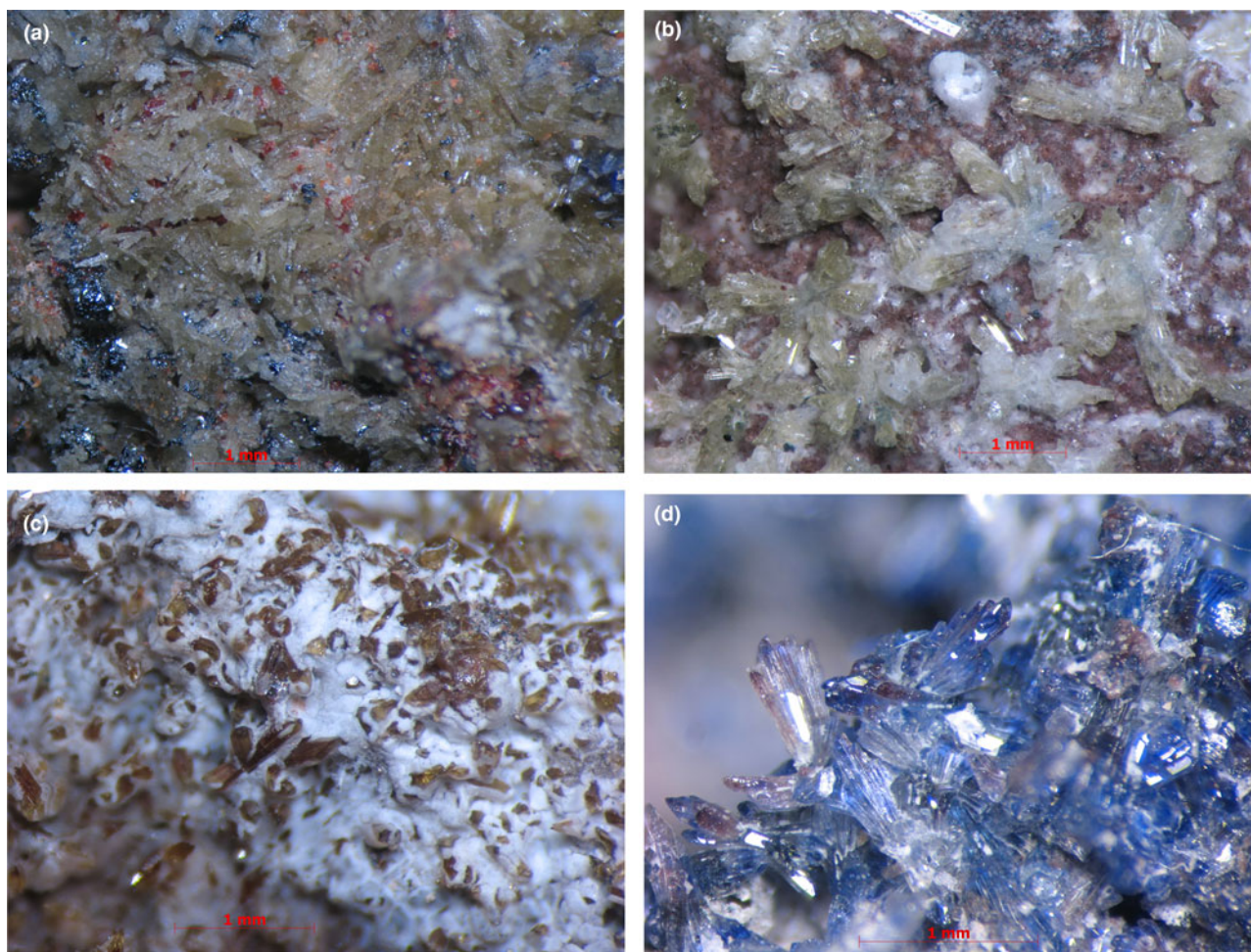


**Fig. 1.** Aggregates of badalovite: (a, sample #4755) crust consisting of crude crystals with red cassiterite and iron-black hematite; (b, sample #4685) radial clusters of prismatic crystals on basalt scoria altered by fumarolic gas; (c, sample #4644) crystal crust partially covered by white apthitalite; and (d, sample #4742) cluster of multicoloured, chemically heterogeneous crystals (red–brown colouration is caused by hematite micro-inclusions, blue areas correspond to zones composed of johillerite; see Fig. 3). FOV width: (a, b) 5.7 mm, (c) 4.4 mm, (d) 3.5 mm. Photo: I.V. Pekov & A.V. Kasatkin.

The new mineral and its name have been approved by the Commission on New Minerals, Nomenclature and Classification of the International Mineralogical Society (IMA), IMA2016–053 (Pekov *et al.*, 2016a). The holotype specimen is deposited in the systematic collection of the Fersman Mineralogical Museum of the Russian Academy of Sciences, Moscow, under the catalogue number 95618.

### Occurrence and general appearance

The general description of the active Arsenatnaya fumarole was given by Pekov *et al.* (2014a, 2018a). Specimens with the new mineral were collected by us from several areas of Arsenatnaya in 2015 (holotype), 2016 and 2017. Temperatures measured using a chromel–alumel thermocouple at the time of collecting in different pockets with badalovite were 380–450°C. It seems that the new mineral was deposited directly from the gas phase as a volcanic sublimate or, more probably, formed as a result of the interaction between fumarolic gas and basalt scoria at a temperature not lower than 450°C. Basalt could be a source of Mg which has very low volatility in such post-volcanic systems at temperatures up to 400–500°C (Symonds and Reed, 1993).

Badalovite is a constituent of fumarolic incrustations mainly consisting of arsenates, sulfates, oxides, chlorides and silicates. It is associated with hematite, tenorite, cassiterite, johillerite, nickenichite, calciojohillerite, bradaczekite, hatertite, magnesiohatertite, metathénardite, apthitalite, langbeinite, calciolangbeinite, sanidine (As-bearing variety), fluorophlogopite, fluororite, tilasite, anhydrite, pseudobrookite, rutile, sylvite, halite, lammerite, urusovite, ericlxmanite, arsmirandite, arsenowagnerite, svabite, popovite, dmisokolovite, shchurovskyite, yurmarinite, krasheninikovite, euchlorine, wulffite, alumoklyuchevskite and sellaitite.

Badalovite forms oblique-angled prismatic crystals (Figs 1 and 2) usually <1 mm long, rarely up to 1 mm × 1 mm × 5 mm. Some crystals are equant. By analogy with other alluaudite-group minerals, it could be assumed that the main forms of badalovite crystals are {100}, {010}, {011} and {201}. Crystals are well-shaped (Fig. 2a) or crude, sometimes divergent, resembling sheaves (Figs 1b and 2b), commonly with numerous inclusions of grains of other minerals or particles of basalt scoria. Some badalovite crystals contain, typically in peripheral parts, zones corresponding chemically to other alluaudite-group arsenates, usually johillerite, nickenichite or calciojohillerite. This zonation commonly has an irregular, spotty character (Fig. 3). Some zoned crystals are

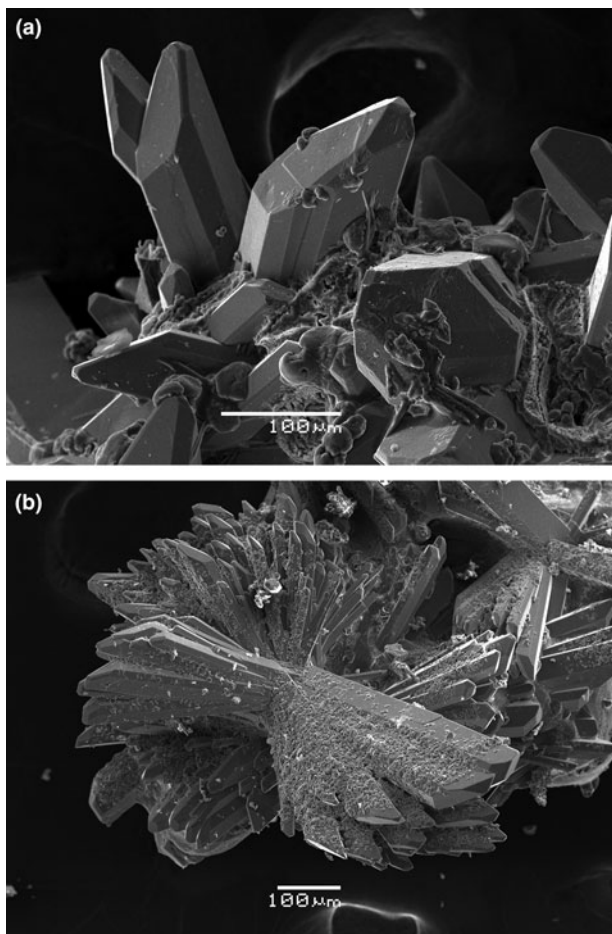


**Fig. 2.** Morphology of badalovite: (a) well-shaped crystals; and (b) sheaf-like clusters of divergent crystals partially covered by fine-grained hematite. Scanning electron microscopy (SEM) secondary electron images.

multi-coloured: parts that correspond chemically to badalovite or calciojohillerite are pale greenish, greenish-yellow or grey; zones of Cu-enriched members of the group, i.e. johillerite or nickenichite, are blue (Fig. 1d). Badalovite crystals are typically combined in groups, open-work clusters, brushes or crusts (Figs 1 and 2) up to several hundred cm<sup>2</sup> in area overgrowing basalt scoria altered by fumarolic gas.

### Physical properties and optical data

Badalovite is transparent, pale green to green, greenish-grey to grey, bluish-greenish, greenish-yellow to bright yellow or honey-yellow, sometimes colourless. The streak is white to pale greenish or pale yellowish and lustre is vitreous. The mineral is brittle. Cleavage or parting was not observed, the fracture is uneven. The Mohs hardness is *ca* 3½. Density was not measured because crystals typically contain abundant mineral inclusions (hematite, cassiterite, different arsenates, etc.) and bubbles. Density calculated for the holotype using the empirical formula is 4.016 g cm<sup>-3</sup>.

In plane polarised transmitted light, badalovite is colourless and non-pleochroic. It is optically biaxial (-),  $\alpha = 1.753(3)$ ,  $\beta = 1.757(3)$ ,  $\gamma = 1.758(3)$  (589 nm),  $2V_{\text{meas.}} = 50(10)^\circ$  (estimated by the curve of the conoscopic figures on the sections perpendicular to the optical axes),  $2V_{\text{calc.}} = 53^\circ$ . Dispersion of optical axes is strong,  $r > v$ . Optical orientation:  $Y = b$ .

### Raman spectroscopy

The Raman spectrum of badalovite (Fig. 4) was obtained on a randomly oriented crystal using an EnSpectr R532 instrument (Dept. of Mineralogy, Moscow State University) with a green laser (532 nm) at room temperature. The output power of the laser beam was ~16 mW. The spectrum was processed using the *EnSpectr* expert mode program in the range from 100 to 4000 cm<sup>-1</sup> with the use of a holographic diffraction grating with 1800 lines cm<sup>-1</sup> and a resolution of 6 cm<sup>-1</sup>. The diameter of the focal spot on the sample was ~10 μm. The backscattered Raman signal was collected with 40× objective, signal acquisition time for a single scan of the spectral range was 1500 ms and the signal was averaged over 10 scans.

The strongest bands in the region 750–950 cm<sup>-1</sup> correspond to As<sup>5+</sup>-O stretching vibrations of AsO<sub>4</sub><sup>3-</sup> anions. A distinct band with a maximum at 561 cm<sup>-1</sup> can be assigned to Fe<sup>3+</sup>-O stretching vibrations. Bands with frequencies lower than 500 cm<sup>-1</sup> correspond to bending vibrations of AsO<sub>4</sub> tetrahedra, Mg-O stretching vibrations and lattice modes. The absence of bands with frequencies higher than 950 cm<sup>-1</sup> indicates the absence of groups with O-H, C-H, C-O, N-H, N-O and B-O bonds in badalovite.

### Chemical composition

The chemical composition of badalovite (Table 1) was determined on a Jeol JSM-6480LV scanning electron microscope equipped

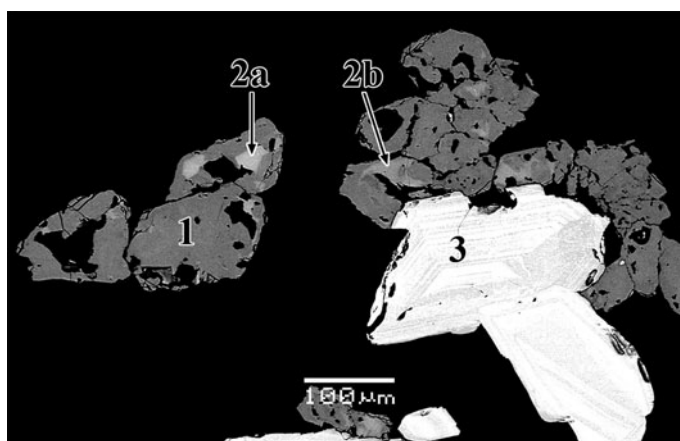


**Fig. 3.** Individual crystals of badalovite (grey: 1) with areas consisting of: johillerite (light grey: 2); 2a - johillerite chemically close to the ideal composition NaCuMg<sub>3</sub>(AsO<sub>4</sub>)<sub>3</sub>; 2b - Cu-depleted johillerite variety; and 3 - intimate intergrowth of cassiterite and hematite. Polished section, SEM back-scatter electron image.

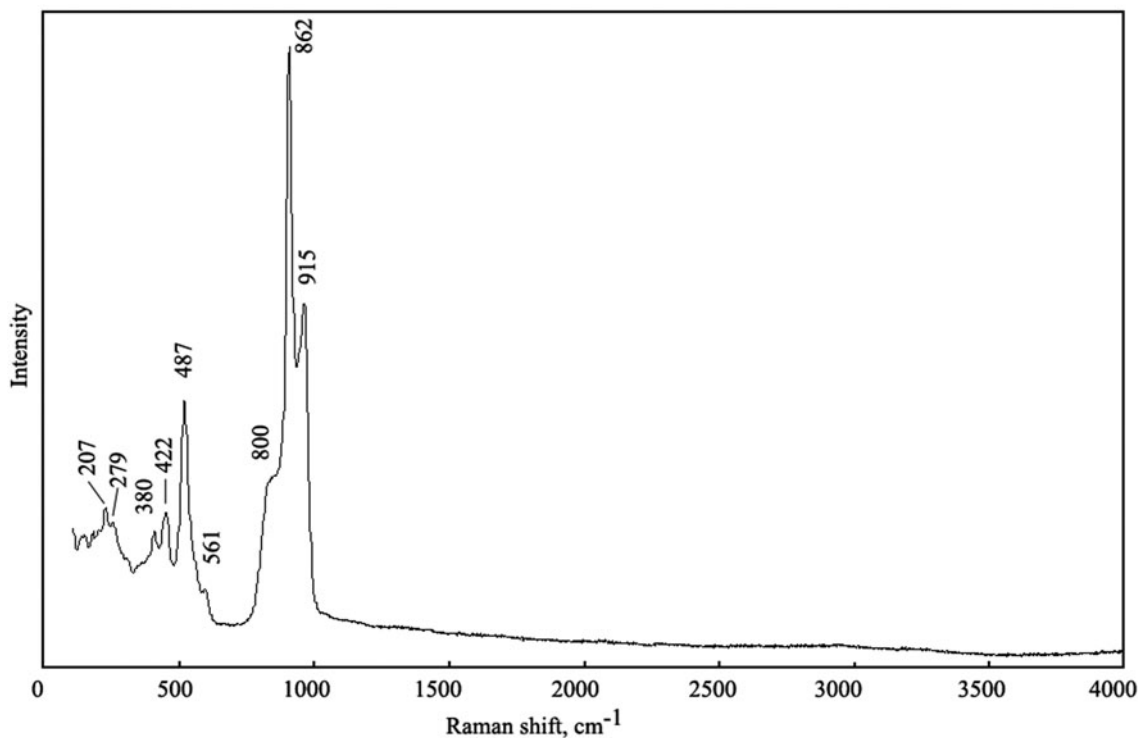


Fig. 4. The Raman spectrum of badalovite.

Table 1. Chemical composition of badalovite.

Sample no.	#4685 (holotype)*	#4644	#4683	#4742 greenish- greyish	#4755	#4791
Colour	pale green	yellow	grey	greenish- greyish	greenish- greyish	green
Wt. %						
Na <sub>2</sub> O	9.23 (9.19–9.31)	8.51	9.45	9.40	9.58	8.89
K <sub>2</sub> O	0.19 (0.15–0.24)	0.12	0.27	0.20	0.21	0.12
CaO	2.04 (1.66–2.85)	2.21	3.00	2.51	1.76	2.19
MgO	13.78 (13.19–14.89)	13.48	14.96	14.02	12.44	13.51
MnO	0.31 (0.24–0.39)	0.70	0.26	0.37	0.32	0.49
CuO	0.12 (0.06–0.17)	0.15	0.87	0.63	0.13	0.30
ZnO	0.24 (0.16–0.27)	0.18	0.44	0.33	0.56	0.31
Al <sub>2</sub> O <sub>3</sub>	0.06 (0.03–0.10)	0.73	0.08	–	0.17	0.83
Fe <sub>2</sub> O <sub>3</sub> **	12.77 (11.38–13.69)	12.56	11.21	11.05	14.45	12.52
TiO <sub>2</sub>	0.01 (0.00–0.05)	–	0.03	0.03	–	–
SiO <sub>2</sub>	0.06 (0.00–0.16)	0.03	0.06	–	–	–
P <sub>2</sub> O <sub>5</sub>	0.33 (0.23–0.62)	0.07	2.76	0.67	0.32	–
V <sub>2</sub> O <sub>5</sub>	0.05 (0.03–0.08)	–	–	0.06	0.04	–
As <sub>2</sub> O <sub>5</sub>	61.51 (60.98–62.87)	61.44	57.76	60.14	61.70	62.83
SO <sub>3</sub>	0.02 (0.00–0.07)	0.03	–	0.03	–	–
Total	100.72	100.21	101.15	99.44	101.68	101.99
Formula calculated on the basis of 12 O apfu						
Na	1.67	1.55	1.69	1.73	1.73	1.59
K	0.02	0.01	0.03	0.02	0.02	0.01
Ca	0.20	0.22	0.30	0.25	0.18	0.22
Mg	1.92	1.89	2.05	1.98	1.73	1.86
Mn	0.02	0.06	0.02	0.03	0.03	0.04
Cu	0.01	0.01	0.06	0.05	0.01	0.02
Zn	0.02	0.01	0.03	0.02	0.04	0.02
Al	0.01	0.08	0.01	–	0.02	0.09
Fe <sup>3+</sup>	0.90	0.89	0.78	0.79	1.01	0.87
Si	0.01	–	0.01	–	–	–
P	0.03	0.01	0.22	0.05	0.03	–
As	3.01	3.02	2.78	2.98	3.01	3.04

\*Average (6 spot analyses, ranges are in parentheses) data for the holotype specimen (sample numbers are field collection numbers). ‘–’ content is below detection limit. \*\*All Fe is calculated as Fe<sup>3+</sup> based on the structure data and considering strongly oxidising conditions of mineral formation in the Arsenatnaya fumarole: only iron minerals with Fe<sup>3+</sup> are found there (Pekov *et al.*, 2014a, 2018a).

with an INCA-Wave 500 wavelength-dispersive spectrometer (Laboratory of Analytical Techniques of High Spatial Resolution, Dept. of Petrology, Moscow State University), with an acceleration voltage of 20 kV, a beam current of 20 nA and a 10 μm beam diameter. The following standards were used: jadeite (Na, Al and Si); KTiOPO<sub>4</sub> (K, Ti and P); wollastonite (Ca); olivine (Mg); MnTiO<sub>3</sub> (Mn); Cu (Cu); ZnS (Zn and S); FeS<sub>2</sub> (Fe); V (V); and GaAs (As). Contents of other elements with atomic numbers higher than carbon are below detection limits. H<sub>2</sub>O was not analysed because both structure data and the Raman spectrum show its absence.

Different coloured samples of badalovite were found to have close chemical composition (Table 1). The empirical formula of the holotype calculated on the basis of 12 O atoms per formula unit (apfu) is Na<sub>1.67</sub>Ca<sub>0.20</sub>K<sub>0.02</sub>Mg<sub>1.92</sub>Zn<sub>0.02</sub>Mn<sub>0.02</sub>Cu<sub>0.01</sub>Fe<sub>0.90</sub><sup>3+</sup>Al<sub>0.01</sub>(As<sub>3.01</sub>P<sub>0.03</sub>Si<sub>0.01</sub>)<sub>Σ3.05</sub>O<sub>12</sub>. The simplified formula is Na<sub>2</sub>Mg<sub>2</sub>Fe<sup>3+</sup>(AsO<sub>4</sub>)<sub>3</sub> which requires Na<sub>2</sub>O 10.93, MgO 14.21, Fe<sub>2</sub>O<sub>3</sub> 14.08, As<sub>2</sub>O<sub>5</sub> 60.78, total 100 wt.%. The end-member formula of the alluaudite supergroup (Hatert, 2019), is NaNaMg(MgFe<sup>3+</sup>)(AsO<sub>4</sub>)<sub>3</sub>.

The correctness of the obtained data is confirmed by the superior value of the Gladstone–Dale compatibility index (Mandarino, 2007):  $1 - (K_p/K_c) = 0.012$ , which is superior.

#### X-ray crystallography and crystal-structure determination

Powder X-ray diffraction data of badalovite (Table 2) were collected with a DRON-2 diffractometer using CuKα radiation. Parameters of the monoclinic unit cell calculated from the powder data are:  $a = 11.89(1)$ ,  $b = 12.799(5)$ ,  $c = 6.667(7)$  Å,  $\beta = 112.48(7)^\circ$  and  $V = 938(2)$  Å<sup>3</sup>.

Single-crystal X-ray studies of badalovite were carried out using an Xcalibur S diffractometer equipped with a CCD detector.

**Table 2.** Powder X-ray diffraction data of badalovite.

$l_{\text{obs}}$	$d_{\text{obs}}$	$l_{\text{calc}}^*$	$d_{\text{calc}}^{**}$	$hkl$
5	8.30	5	8.336	110
<b>38</b>	<b>6.41</b>	30	6.392	020
2	5.865	3	5.826	$\bar{1}11$
<b>20</b>	<b>5.505</b>	20	5.498	200
12	4.388	15	4.381	111
11	4.171	9	4.168	220
16	4.040	20	4.038	$\bar{2}21$
2	3.972	2	3.973	130
11	3.705	20	3.701	$\bar{3}11$
<b>23</b>	<b>3.577</b>	32	3.571	$\bar{1}31$
<b>25</b>	<b>3.523</b>	26	3.523	310
3	3.302	2	3.272	$\bar{2}02$
<b>46</b>	<b>3.211</b>	57, 9	3.205, 3.196	$\bar{1}12, 040$
6	3.150	7	3.146	131
17	3.072	11, 14	3.078, 3.063	002, 221
<b>28</b>	<b>2.911</b>	11, 34	2.913, 2.908	$\bar{2}22, \bar{3}12$
15	2.834	19	2.836	041
<b>100</b>	<b>2.765</b>	12, 8, 100, 40	2.779, 2.773, 2.763, 2.749	330, 022, 240, 400
6	2.694	7	2.693	$\bar{4}21$
17	2.647	25	2.648	112
<b>26</b>	<b>2.618</b>	45	2.615	$\bar{1}32$
14	2.525	7	2.525	420
4	2.334	3, 3	2.340, 2.332	$\bar{5}11, 202$
5	2.295	5	2.295	331
8	2.173	4, 11	2.175, 2.167	441, 510
7	2.098	9	2.097	350
4	2.018	6, 4	2.024, 2.013	$\bar{1}52, 061$
8	1.986	2, 17	1.984, 1.983	312, $\bar{5}32$
6	1.954	5, 3	1.954, 1.954	530, 023
8	1.859	11	1.859	152
8	1.819	18	1.817	332
4	1.759	7	1.759	$\bar{1}71$
2	1.733	1, 4, 2	1.736, 1.731, 1.728	443, $\bar{4}61, 133$
2	1.703	2, 4	1.703, 1.700	531, 171
7	1.666	2, 2, 4	1.670, 1.670, 1.667	$\bar{7}12, \bar{7}11, 550$
12	1.657	27, 12	1.656, 1.654	204, $\bar{6}42$
9	1.590	16	1.590	640
8	1.561	2, 1, 4, 12	1.564, 1.559, 1.559, 1.558	514, $\bar{7}13, 710, \bar{3}72$
3	1.540	1, 4	1.539, 1.539	004, $\bar{2}63$
9	1.516	8, 12	1.517, 1.514	371, 172
4	1.487	4, 8	1.493, 1.484	$\bar{6}04, \bar{8}02$
5	1.474	2, 3, 7, 1	1.478, 1.474, 1.474, 1.470	534, $\bar{7}33, 730, \bar{2}44$
5	1.458	1, 13, 4	1.460, 1.456, 1.453	333, $\bar{4}44, 281$
4	1.404	1, 5, 4, 4	1.407, 1.407, 1.405, 1.400	481, $\bar{7}52, 570, \bar{3}73$
4	1.388	3, 12	1.387, 1.386	$\bar{8}23, 044$

\*For the calculated pattern, only reflections with intensities  $\geq 1$  are given. \*\*For the unit-cell parameters calculated from single-crystal data. The strongest reflections are marked in boldtype.

The crystal structure was solved by direct methods and refined with the use of the *SHELX-97* software package (Sheldrick, 2008) to  $R_1 = 0.0249$  on the basis of 1538 independent reflections with  $I > 2\sigma(I)$ . Crystal data, data collection information and structure refinement details are given in Table 3, coordinates and thermal displacement parameters of atoms and bond-valence sums in Table 4 and selected interatomic distances in Table 5. The crystallographic information files have been deposited with the Principal Editor of *Mineralogical Magazine* and are available as Supplementary material (see below).

## Discussion

Badalovite is a mineral of the alluaudite group belonging to the alluaudite supergroup and the cation sites in its structure are labelled below in accordance with the nomenclature of this supergroup (Hatert, 2019).

**Table 3.** Crystal data, data collection information and structure refinement details for badalovite.

Formula derived from structure refinement	$A^{(1)}(\text{Na}_{0.80}\text{Ca}_{0.20})^{A(2)'}(\text{Na}_{0.90}\square_{0.10})^{M(1)}(\text{Mg}_{0.85}\text{Ca}_{0.15})^{M(2)}(\text{Mg}_{1.08}\text{Fe}_{0.92}^{3+})(\text{AsO}_4)_3$
Formula weight	568.17
Temperature (K)	293(2)
Radiation and wavelength (Å)	MoK $\alpha$ , 0.71073
Crystal system, space group, Z	Monoclinic, C2/c, 4
Unit-cell dimensions $a, b, c$ (Å); $\beta$ (°)	11.9034(3), 12.7832(2), 6.66340(16); 112.523(3)
$V$ (Å <sup>3</sup> )	936.59(4)
Absorption coefficient $\mu$ (mm <sup>-1</sup> )	12.476
$F_{000}$	1069
Crystal size (mm)	0.05 × 0.09 × 0.12
Diffractometer	Xcalibur S CCD
$\theta$ range for data collection (°)	3.187–32.507
Index ranges	$-17 \leq h \leq 17, -19 \leq k \leq 19, -9 \leq l \leq 9$
Reflections collected	7674
Independent reflections	1165 ( $R_{\text{int}} = 0.0228$ )
Independent reflections with $I > 2\sigma(I)$	1130
Data reduction	<i>CrysAlisPro, version 1.171.37.35</i> (Agilent, 2014)
Absorption correction	Gaussian [Numerical absorption correction based on Gaussian integration over a multifaceted crystal model]
Structure solution	Direct methods
Refinement method	Full-matrix least-squares on $F^2$
Number of refined parameters	99
Final $R$ indices [ $I > 2\sigma(I)$ ]	$R_1 = 0.0208, wR_2 = 0.0448$
$R$ indices (all data)	$R_1 = 0.0223, wR_2 = 0.0453$
GoF	1.175
Largest diff. peak and hole, $e^-/\text{Å}^3$	0.94 and -0.49

The crystal structure of badalovite (Fig. 5a), like structures of other members of the alluaudite group (Moore, 1971; Moore and Ito, 1979; Krivovichev *et al.*, 2013; Hatert, 2019 and references therein), contains zig-zag chains of edge-sharing  $M(1)\text{O}_6$  and  $M(2)\text{O}_6$  octahedra. The  $M$ -octahedral chains consist of  $[M(2)_2\text{O}_{10}]$  dimers of distorted  $M(2)\text{O}_6$  octahedra connected via distorted  $M(1)\text{O}_6$  octahedra that are isolated from one another. As(1) $\text{O}_4$  tetrahedra share all vertices with the  $M$ -centred octahedra forming the (010) heteropolyhedral layers while each As(2) $\text{O}_4$  tetrahedron shares three vertices with the  $M$ -centred octahedra of one layer (Fig. 5b) and the fourth vertex with the octahedron of adjacent layer, thus linking the layers to a three-dimensional

**Table 4.** Coordinates and equivalent displacement parameters ( $U_{\text{eq}}$ , in Å<sup>2</sup>) of atoms, bond-valence sums (BVS) and site multiplicities ( $Q$ ) for badalovite.

Site*	$x$	$y$	$z$	$U_{\text{eq}}$	BVS**	$Q$
A(1)	½	0	0	0.0176(7)	1.150	4
A(2)'	0	-0.0074(2)	¼	0.0300(9)	0.758	4
M(1)	0	0.26575(10)	¼	0.0085(5)	2.072	4
M(2)	0.28506(5)	0.65664(4)	0.37552(9)	0.0061(2)	2.436	8
As(1)	0	0.71125(3)	¼	0.00565(11)	4.992	4
As(2)	0.23428(3)	0.88794(2)	0.12259(4)	0.00589(10)	5.063	8
O(1)	0.46104(19)	0.71525(16)	0.5226(3)	0.0096(4)	1.994	8
O(2)	0.1098(2)	0.62614(16)	0.2591(4)	0.0126(4)	1.958	8
O(3)	0.3396(2)	0.67018(16)	0.1209(3)	0.0095(4)	2.030	8
O(4)	0.11706(19)	0.39678(16)	0.3179(3)	0.0111(4)	2.083	8
O(5)	0.21719(19)	0.81598(16)	0.3222(3)	0.0089(4)	1.935	8
O(6)	0.3345(2)	0.50431(16)	0.3932(3)	0.0115(4)	1.986	8

\*For occupancies of the A and M sites see Table 3. \*\*Bond-valence parameters are taken from Gagné and Hawthorne (2015). All calculations were done taking into account given cation distribution.

**Table 5.** Selected interatomic distances (Å) in the structure of badalovite.

A(1)–O(2)	2.358(2)	<i>M(1)–O(4)</i>	2.114(2)	As(1)–O(2)	1.684(2)
A(1)–O(4)	2.431(2)	<i>M(1)–O(1)</i>	2.139(2)	As(1)–O(1)	1.690(2)
A(1)–O(4)	2.540(2)	<i>M(1)–O(3)</i>	2.150(2)	<As(1)–O>	1.687
A(1)–O(2)	2.914(2)	< <i>M(1)–O</i> >	2.134		
<A(1)–O>	2.561			As(2)–O(4)	1.662(2)
		<i>M(2)–O(2)</i>	1.966(2)	As(2)–O(6)	1.682(2)
A(2)'–O(6)	2.439(2)	<i>M(2)–O(6)</i>	2.025(2)	As(2)–O(3)	1.692(2)
A(2)'–O(6)	2.501(2)	<i>M(2)–O(3)</i>	2.042(2)	As(2)–O(5)	1.693(2)
A(2)'–O(3)	2.878(3)	<i>M(2)–O(5)</i>	2.055(2)	<As(2)–O>	1.682
A(2)'–O(1)	3.005(3)	<i>M(2)–O(1)</i>	2.083(2)		
<A(2)'–O>	2.706	<i>M(2)–O(5)</i>	2.170(2)		
		< <i>M(2)–O</i> >	2.057		

Elongated A(1)–O distances are given in italics.

framework (Fig. 5a). In badalovite Mg strongly prevails in the M(1) site (Wyckoff symbol: 4e) whereas the M(2) site (8f) contains approximately equal amounts of Mg and Fe<sup>3+</sup>. The presence of Fe in a trivalent state is undoubtedly confirmed by the mean M(2)–O distance [2.056 Å, whereas mean M(1)–O distance is 2.134; Table 5] and bond-valence sum (2.49, Table 4). This is in agreement with the strongly oxidising conditions of mineral deposition in the Arsenatnaya fumarole (see above).

Channels of two types in the framework contain the A(1) and A(2)' sites predominantly occupied by Na in badalovite. The A(1)

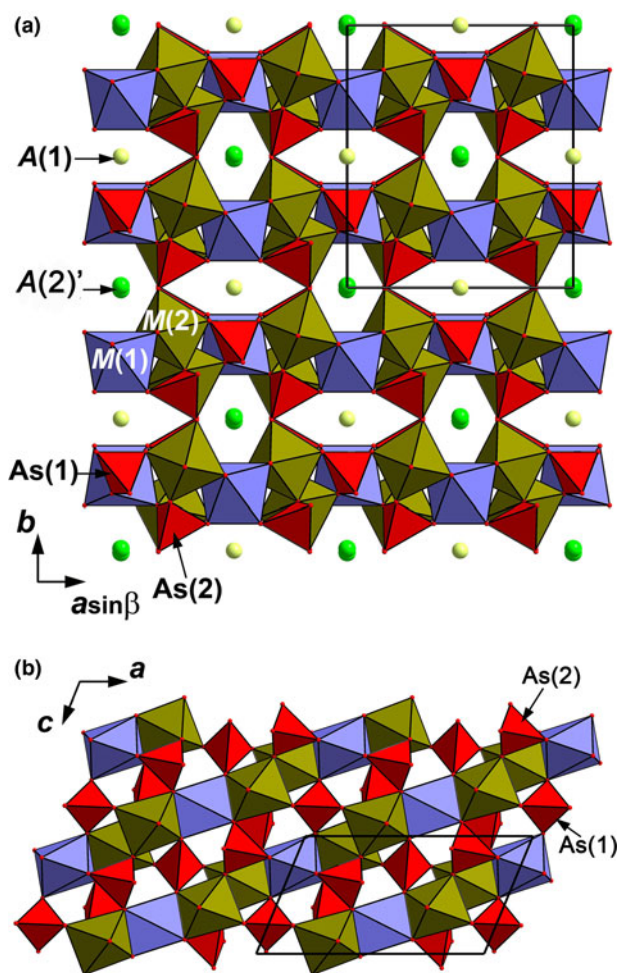


**Fig. 5.** The crystal structure of badalovite (a) projected along *c* and (b) the heteropolyhedral layer in it. For legend see Tables 4 and 5. The unit cell is outlined.

site is coordinated by six O atoms with the distances in the range from 2.357(2) to 2.540(2) Å, two elongated A(1)–O(2) bonds [2.916(2) Å] could also be included in the coordination sphere of A(1). The A(2)' site centres eight-fold oxygen polyhedron with A(2)'–O distances in the range from 2.437(2) to 3.005(3) Å (Table 5). A minor admixture of Cu (0.01 apfu) found by electron microprobe could be located in M(2) or in the A(1)' site that typical for Cu<sup>2+</sup> cations in alluaudite-type arsenates (Krivovichev *et al.*, 2013; Koshlyakova *et al.*, 2018; Hatert, 2019): a small peak with  $x = 0.0$ ,  $y = 0.5072$  and  $z = 0.25$  on the residual Fourier synthesis ( $1.02 e^-/\text{Å}^3$ ) revealed during the refinement of the badalovite structure corresponds to the A(1)' site.

The formula of the crystal studied derived from structure refinement is  $A^{(1)}(\text{Na}_{0.80}\text{Ca}_{0.20})^{A(1)'}\square^{A(2)'}\square^{A(2)'}$  ( $\text{Na}_{0.90}\square_{0.10}$ )  $M^{(1)}(\text{Mg}_{0.85}\text{Ca}_{0.15})^{M(2)}(\text{Mg}_{1.08}\text{Fe}_{0.92}^{3+})(\text{AsO}_4)_3$  ( $\square$  – vacancy). The simplified crystal chemical formula of badalovite can be written as  $A^{(1)}\text{Na}^{A(1)'}\square^{A(2)'}\square^{A(2)'}\text{Na}^{M(1)}\text{Mg}^{M(2)}(\text{Mg}_{0.5}\text{Fe}_{0.5}^{3+})_2(\text{AsO}_4)_3$ , or, in the shortened form,  $A[\text{NaNa}]^M[\text{Mg}(\text{MgFe}^{3+})](\text{AsO}_4)_3$  ( $Z = 4$ ).

Another alluaudite-group arsenate, yazganite (Sarp and Černý, 2005) has the same species-defining cations as badalovite, however, (1) yazganite is a hydrous mineral and (2) the cation ratios in these minerals are significantly different. The simplified crystal chemical formula of yazganite is  $A^{(1)}\text{Na}^{A(1)'}\square^{A(2)'}\square^{A(2)'}$  ( $\text{H}_2\text{O}$ )  $M^{(1)}\text{Mg}^{M(2)}(\text{Fe}^{3+})_2(\text{AsO}_4)_3$  and its end-member formula, according to the actual nomenclature of the alluaudite supergroup, is  $\text{NaMgFe}_2^{3+}(\text{AsO}_4)_3 \cdot \text{H}_2\text{O}$  (Hatert, 2019).

**Acknowledgements.** We thank an anonymous referee, Oleg Siidra and Structures Editor Daniel Atencio for valuable comments. This study was supported by the Russian Science Foundation, grant no. 19-17-00050.

**Supplementary material.** To view supplementary material for this article, please visit <https://doi.org/10.1180/mgm.2020.43>.

## References

- Agilent Technologies (2014) *CrysAlisPro Software system, version 1.171.37.35*. Agilent Technologies UK Ltd, Oxford, UK.
- Gagné O.C., and Hawthorne F.C. (2015) Comprehensive derivation of bond-valence parameters for ion pairs involving oxygen. *Acta Crystallographica*, **B71**, 562–578.
- Hatert F. (2019) A new nomenclature scheme for the alluaudite supergroup. *European Journal of Mineralogy*, **31**, 807–822.
- Koshlyakova N.N., Zubkova N.V., Pekov I.V., Giester G. and Sidorov E.G. (2018) Crystal chemistry of johillerite. *The Canadian Mineralogist*, **56**, 189–201.
- Krivovichev S.V., Vergasova L.P., Filatov S.K., Rybin D.S., Britvin S.N. and Ananiev V.V. (2013) Hatertite,  $\text{Na}_2(\text{Ca},\text{Na})(\text{Fe}^{3+},\text{Cu})_2(\text{AsO}_4)_3$ , a new alluaudite-group mineral from Tolbachik fumaroles, Kamchatka peninsula, Russia. *European Journal of Mineralogy*, **25**, 683–691.
- Mandarino J.A. (2007) The Gladstone–Dale compatibility of minerals and its use in selecting mineral species for further study. *The Canadian Mineralogist*, **45**, 1307–1324.
- Moore P.B. (1971) Crystal-chemistry of alluaudite structure type – contribution to paragenesis of pegmatite phosphate giant crystals. *American Mineralogist*, **56**, 1955–1975.
- Moore P.B. and Ito J. (1979) Alluaudites, wyllieites, arrojadites: Crystal chemistry and nomenclature. *Mineralogical Magazine*, **43**, 227–235.
- Pekov I.V., Zubkova N.V., Yapaskurt V.O., Belakovskiy D.I., Lykova I.S., Vigasina M.F., Sidorov E.G. and Pushcharovsky D.Yu. (2014a) New arsenate minerals from the Arsenatnaya fumarole, Tolbachik volcano, Kamchatka, Russia. I. Yurmarinite,  $\text{Na}_7(\text{Fe}^{3+},\text{Mg},\text{Cu})_4(\text{AsO}_4)_6$ . *Mineralogical Magazine*, **78**, 905–917.
- Pekov I.V., Zubkova N.V., Yapaskurt V.O., Belakovskiy D.I., Vigasina M.F., Sidorov E.G. and Pushcharovsky D.Yu. (2014b) New arsenate minerals from the Arsenatnaya fumarole, Tolbachik volcano, Kamchatka, Russia.

- II. Ericlaxmanite and kozyrevskite, two natural modifications of  $\text{Cu}_4\text{O}(\text{AsO}_4)_2$ . *Mineralogical Magazine*, **78**, 1527–1543.
- Pekov I.V., Zubkova N.V., Yapaskurt V.O., Belakovskiy D.I., Vigasina M.F., Sidorov E.G. and Pushcharovsky D.Yu. (2015a) New arsenate minerals from the Arsenatnaya fumarole, Tolbachik volcano, Kamchatka, Russia. III. Popovite,  $\text{Cu}_5\text{O}_2(\text{AsO}_4)_2$ . *Mineralogical Magazine*, **79**, 133–143.
- Pekov I.V., Zubkova N.V., Belakovskiy D.I., Yapaskurt V.O., Vigasina M.F., Sidorov E.G. and Pushcharovsky D.Yu. (2015b) New arsenate minerals from the Arsenatnaya fumarole, Tolbachik volcano, Kamchatka, Russia. IV. Shchurovskiyite,  $\text{K}_2\text{CaCu}_6\text{O}_2(\text{AsO}_4)_4$ , and dmsokolovite,  $\text{K}_3\text{Cu}_5\text{AlO}_2(\text{AsO}_4)_4$ . *Mineralogical Magazine*, **79**, 1737–1753.
- Pekov I.V., Koshlyakova N.N., Agakhanov A.A., Zubkova N.V., Belakovskiy D.I., Vigasina M.F., Turchkova A.G., Sidorov E.G., Pushcharovsky D.Y. (2016a) Badalovite, IMA 2016-053. CNMNC Newsletter No. 33, October 2016, page 1140; *Mineralogical Magazine*, **80**, 1135–1144.
- Pekov I.V., Yapaskurt V.O., Britvin S.N., Zubkova N.V., Vigasina M.F. and Sidorov E.G. (2016b) New arsenate minerals from the Arsenatnaya fumarole, Tolbachik volcano, Kamchatka, Russia. V. Katiarsite,  $\text{KTiO}(\text{AsO}_4)$ . *Mineralogical Magazine*, **80**, 639–646.
- Pekov I.V., Zubkova N.V., Yapaskurt V.O., Polekhovskiy Yu.S., Vigasina M.F., Belakovskiy D.I., Britvin S.N., Sidorov E.G. and Pushcharovsky D.Yu. (2016c) New arsenate minerals from the Arsenatnaya fumarole, Tolbachik volcano, Kamchatka, Russia. VI. Melanarsite,  $\text{K}_3\text{Cu}_7\text{Fe}^{3+}\text{O}_4(\text{AsO}_4)_4$ . *Mineralogical Magazine*, **80**, 855–867.
- Pekov I.V., Yapaskurt V.O., Belakovskiy D.I., Vigasina M.F., Zubkova N.V. and Sidorov E.G. (2017) New arsenate minerals from the Arsenatnaya fumarole, Tolbachik volcano, Kamchatka, Russia. VII. Pharmazincite,  $\text{KZnAsO}_4$ . *Mineralogical Magazine*, **81**, 1001–1008.
- Pekov I.V., Koshlyakova N.N., Zubkova N.V., Lykova I.S., Britvin S.N., Yapaskurt V.O., Agakhanov A.A., Shchipalkina N.V., Turchkova A.G. and Sidorov E.G. (2018a) Fumarolic arsenates – a special type of arsenic mineralization. *European Journal of Mineralogy*, **30**, 305–322.
- Pekov I.V., Zubkova N.V., Agakhanov A.A., Yapaskurt V.O., Chukanov N.V., Belakovskiy D.I., Sidorov E.G. and Pushcharovsky D.Yu. (2018b) New arsenate minerals from the Arsenatnaya fumarole, Tolbachik volcano, Kamchatka, Russia. VIII. Arsenowagnerite,  $\text{Mg}_2(\text{AsO}_4)\text{F}$ . *Mineralogical Magazine*, **82**, 877–888.
- Pekov I.V., Zubkova N.V., Agakhanov A.A., Belakovskiy D.I., Vigasina M.F., Yapaskurt V.O., Sidorov E.G., Britvin S.N. and Pushcharovsky D.Y. (2019a) New arsenate minerals from the Arsenatnaya fumarole, Tolbachik volcano, Kamchatka, Russia. IX. Arsenatrotitanite,  $\text{NaTiO}(\text{AsO}_4)$ . *Mineralogical Magazine*, **83**, 453–458.
- Pekov I.V., Zubkova N.V., Agakhanov A.A., Ksenofontov D.A., Pautov L.A., Sidorov E.G., Britvin S.N., Vigasina M.F. and Pushcharovsky D.Yu. (2019b) New arsenate minerals from the Arsenatnaya fumarole, Tolbachik volcano, Kamchatka, Russia. X. Edtollite,  $\text{K}_2\text{NaCu}_5\text{Fe}^{3+}\text{O}_2(\text{AsO}_4)_4$ , and alumoedtollite,  $\text{K}_2\text{NaCu}_5\text{AlO}_2(\text{AsO}_4)_4$ . *Mineralogical Magazine*, **83**, 485–495.
- Pekov I.V., Lykova I.S., Yapaskurt V.O., Belakovskiy D.I., Turchkova A.G., Britvin S.N., Sidorov E.G. and Scheidl K.S. (2019c) New arsenate minerals from the Arsenatnaya fumarole, Tolbachik volcano, Kamchatka, Russia. XI. Anatolyite,  $\text{Na}_6(\text{Ca,Na})(\text{Mg,Fe}^{3+})_3\text{Al}(\text{AsO}_4)_6$ . *Mineralogical Magazine*, **83**, 633–638.
- Pekov I.V., Lykova I.S., Agakhanov A.A., Belakovskiy D.I., Vigasina M.F., Britvin S.N., Turchkova A.G., Sidorov E.G. and Scheidl K.S. (2019d) New arsenate minerals from the Arsenatnaya fumarole, Tolbachik volcano, Kamchatka, Russia. XII. Zubkovaite,  $\text{Ca}_3\text{Cu}_3(\text{AsO}_4)_4$ . *Mineralogical Magazine*, **83**, 879–886.
- Pekov I.V., Zubkova N.V., Koshlyakova N.N., Agakhanov A.A., Belakovskiy D.I., Vigasina M.F., Yapaskurt V.O., Britvin S.N., Turchkova A.G., Sidorov E.G., Pushcharovsky D.Y. (2020) New arsenate minerals from the Arsenatnaya fumarole, Tolbachik volcano, Kamchatka, Russia. XIII. Pansnerite,  $\text{K}_3\text{Na}_3\text{Fe}_6^{3+}(\text{AsO}_4)_8$ . *Mineralogical Magazine*, **84**, 143–151.
- Sarp H. and Černý R. (2005) Yazganite,  $\text{NaFe}_2^{3+}(\text{Mg,Mn})(\text{AsO}_4)_3 \cdot \text{H}_2\text{O}$ , a new mineral: its description and crystal structure. *European Journal of Mineralogy*, **17**, 367–374.
- Sheldrick G.M. (2008) A short history of SHELX. *Acta Crystallographica*, **A64**, 112–122.
- Symonds R.B. and Reed M.H. (1993) Calculation of multicomponent chemical equilibria in gas–solid–liquid systems: calculation methods, thermochemical data, and applications to studies of high-temperature volcanic gases with examples from Mount St. Helens. *American Journal of Science*, **293**, 758–864.